Excited-State Potential Energy Curves from Time-Dependent Density-Functional Theory: A Cross Section of Formaldehyde's $^1A_1$ Manifold

MARK E. CASIDA, KIM C. CASIDA, DENNIS R. SALAHUB

Département de Chimie, Université de Montréal, C.P. 6128, Succursale centre-ville, Montréal, Québec H3C 3J7, Canada

ABSTRACT: This work reports the first density-functional theory (DFT) treatment of excited-state potential energy surfaces exhibiting avoided crossings. Time-dependent DFT (TD-DFT) results, using a recently proposed asymptotically corrected local density approximation functional, are compared with multireference doubles configuration interaction (MRD-CI) results for the $^1A_1$ manifold of the CO stretching curves of planar formaldehyde. TD-DFT is found to reproduce the qualitative features essential for understanding the spectroscopy of this manifold, specifically the strong mixing of the $^1(\pi, \pi^*)$ with Rydberg transitions and the resultant avoided crossings. © 1998 John Wiley & Sons, Inc. Int J Quant Chem 70: 933–941, 1998

Key words: time-dependent density-functional theory; excited state surfaces; avoided crossings

1. Introduction

The well-established place of photochemistry within the greater domain of chemistry stems from the fact that different reaction pathways are available, and different products may be obtained,

from photochemical as opposed to thermal processes. Photochemical pathways are important in synthesis, in state-selective chemistry, in decomposition of chemicals released into the environment, and in the pursuit of materials with novel optical properties. A detailed understanding of photochemical reactions begins with an understanding of the manifold of excited-state potential energy surfaces of the molecular species involved. The very features which can make the description of these surfaces difficult are also the ones which are important for photochemistry: the number and

density of states and their various types of encounters (i.e., crossings, avoided crossings, conical intersections.) These encounter regions are of particular interest because, for example, avoided crossings significantly alter the shapes of the adiabatic surfaces.

Clearly the theoretical methods used to calculate excited-state surfaces need to be capable of describing the interactions between surfaces in the encounter regions, and correctly reproducing the resultant shapes of the surfaces. While some avoided crossings are simply due to avoided crossings at the orbital level, many are due to configuration mixing at the n-electron level and thus require a theoretical method capable of describing this mixing. Various correlated ab initio methods can handle this. However, production of multiple excited-state surfaces is a computationally demanding task, and this is especially true for the medium and large sized molecules of interest for practical applications. Thus, an inexpensive yet accurate method which could obtain such avoided crossings would be very useful.

Hohenberg–Kohn–Sham density-functional theory (DFT) [1, 2] has proven remarkably successful at providing a variety of ground-state properties to an accuracy comparable to that of correlated ab initio methods, at a fraction of the computational cost. Thus, the ability to study the structure of excited-state surfaces via DFT would be valuable. However, the DFT treatment of excited states is not yet as fully developed as is the ground-state theory. To our knowledge, no previously published study using any DFT method has ever reported an avoided crossing due to configuration mixing.

In molecular applications of DFT, excited states have traditionally been treated by simply applying ground-state DFT to excited states. This is based, in the first instance, on the theorem that the energy of the lowest excited state of each symmetry may be obtained by minimizing a functional of its charge density ([3] pp. 204–205) and is, for example, the usual way to treat the lowest triplet excited state of a closed-shell molecule in DFT. Excitation energies are then simply obtained by the ΔSCF (self-consistent field) or related transition orbital method. This same approach is often applied with impunity to treat higher excited states. Another formal problem (usually ignored) is that the functional needed for each excited state need not be the same as that used for the ground state. However, the primary difficulty with this method

is practical as well as formal. The so-called excited-state multiplet problem originates in the intrinsic limitation to n-occupied Kohn–Sham orbitals when constructing excited-state wave functions. This is frequently insufficient to construct open-shell reference wave functions such as in the very simple and notable case of singlet excited states of a closed-shell molecule where $n + 2$ orbitals are actually needed to construct the singlet wave function, $\Phi \rightarrow (1/\sqrt{2})(\hat{a}_{a\uparrow}^\dagger \hat{a}_{i\downarrow} + \hat{a}_{a\downarrow}^\dagger \hat{a}_{i\uparrow})\Phi$. A group-theoretic method has been devised which partially addresses this problem, but it is, of course, not able to describe important configuration mixing arising from other effects besides symmetry [4–7]. In cases where nonsymmetry-related mixing of configurations is expected, e.g., based on experimental results, a *post hoc* configuration-interaction-like correction can sometimes be applied (e.g., [8] p. 5025) at the risk of double counting correlation effects. However, this is of limited utility for predictive purposes, and it is clearly not a very natural, nor well justified, way to treat the structure of excited-state surfaces where avoided crossings involving configuration mixing are important.

For atoms and simplified cluster models, photoabsorbtion spectra have long been calculated using a time-dependent generalization of the Kohn–Sham equation,

$$\left(-\frac{1}{2}\nabla^2 + v(\mathbf{r}, t) + \int \frac{\rho(\mathbf{r}, t)}{|\mathbf{r} - \mathbf{r}'|} \, d\mathbf{r}' + v_{xc}[\rho_t](\mathbf{r}) \right)$$
$$\times \psi_j(\mathbf{r}, t) = i\frac{\partial}{\partial t}\psi_j(\mathbf{r}, t), \tag{1.1}$$

within the adiabatic approximation. Here $v_{xc}[\rho_t](\mathbf{r}) = \delta E_{xc}/\delta\rho_t(\mathbf{r})$, where $\rho_t(\mathbf{r}) = \rho(\mathbf{r}, t)$. In this approach, a scattering theory formalism is used, and spectra are obtained in the form of a spectral strength function [9–16]. This scattering theory approach precludes the treatment of spectroscopically dark states, and, although it is a natural way to treat the continuum part of the spectrum, artificial line broadening is required for treatment of the discrete spectrum.

Although time-dependent DFT (TD-DFT) was initially *ad hoc*, a substantial body of work has now given it a rigorous formal footing [17–26] (see especially reviews by Gross and co-workers [27–29]). The dynamic response of the charge density for a system, initially in its ground stationary state, that is exposed to a time-dependent perturbation, is described via the time-dependent

Kohn–Sham equation (1.1). Excitation energies, ω_I, and oscillator strengths, f_I, may then be obtained from the poles and residues of the dynamic polarizability,

$$\bar{\alpha}(\omega) = \sum_I \frac{f_I}{\omega_I^2 - \omega^2}, \tag{1.2}$$

using the well-known sum-over-states theorem [30]. We have formulated [30] and implemented [31] this approach in a manner suitable for molecular applications. The excitation energies and oscillator strengths, respectively, are the eigenvalues and eigenvectors obtained by solving a matrix eigenvalue problem,

$$\Omega \mathbf{F}_I = \omega_I^2 \mathbf{F}_I, \tag{1.3}$$

where (in the spin density formalism)

$$\begin{aligned}
\Omega_{ia\sigma, jb\tau} = {} & \delta_{\sigma\tau}\delta_{ij}\delta_{ab}(\epsilon_{a\sigma} - \epsilon_{i\sigma})^2 \\
& + \sqrt{\epsilon_{a\sigma} - \epsilon_{i\sigma}}\,[ia \,|\, \delta V_{\mathrm{SCF}}^\sigma / \delta\rho_\tau \,|\, jb] \\
& \times \sqrt{\epsilon_{b\tau} - \epsilon_{j\tau}}
\end{aligned} \tag{1.4}$$

[30–32] is constructed from the Kohn–Sham orbitals and orbital energies for the unperturbed self-consistent field problem (i.e., calculated in the SCF step). This provides a natural way to treat discrete spectra and yields dark as well as bright states. It should be emphasized that Eq. (1.3) is completely rigorous, involving no further approximations beyond the finite basis set model and the functionals used in TD-DFT. In the adiabatic approximation, which will be used in this work, Ω is independent of ω, so this is an ordinary eigenvalue problem. (See Ref. [30] for a discussion of the nonadiabatic case.) The presence of configuration mixing in this method follows from the configuration interaction (CI)-like nature of Eq. (1.3) as does the ability to generate entire manifolds of excitation energies in a one-shot process. This method is thus a natural candidate for a computationally simple treatment of excited-state surfaces.

In order for TD-DFT to be able to describe, even qualitatively, surfaces exhibiting avoided crossings due to configuration mixing, two factors are important: (1) the structure of the TD-DFT coupling matrix ($\delta V_{\mathrm{SCF}}/\delta\rho$) and (2) the functional. Although our formulation of TD-DFT resembles time-dependent Hartree–Fock (TDHF), the TD-DFT coupling matrix differs significantly from that of TDHF (see Ref. [30]). TD-DFT appears to do quite well at describing the configuration mixing responsible for multiplet splittings, in which case the mixing is due primarily to symmetry [31, 33]. We have also noted the occurrence of significant configuration mixing that does not arise from symmetry [31], however, its correctness has not been examined explicitly. A severe test is to see whether TD-DFT can describe the strong configuration mixing responsible for avoided crossings. The present study demonstrates that TD-DFT can give at least a qualitatively correct description in the difficult case of avoided crossings due to mixing of valence and Rydberg excitations in the $^1A_1$ manifold of formaldehyde.

The simultaneous description of valence and Rydberg excitations is a demanding task for the functional. The TD-DFT method has been found to give remarkably good results for low-lying vertical excitations, when the local density approximation (LDA) is used [31, 33, 34]. We have also shown that correction of the asymptotic behavior of the exchange–correlation potential, v_{xc}, used in the SCF step, is crucial for treating higher excitations [33]. Quite reasonable results are obtained by using the asymptotically correct potential of van Leeuwen and Baerends [35] in the SCF step, combined with the time-dependent local density approximation (TDLDA) for the post-SCF step [33, 36]. We have improved on this by combining the LB94 potential in the asymptotic region with the LDA in the "bulk" region of the molecule where $v_{\mathrm{xc}}^{\mathrm{LDA}}$ is more nearly parallel to the exact potential than is $v_{\mathrm{xc}}^{\mathrm{LB94}}$, while at the same time shifting $v_{\mathrm{xc}}^{\mathrm{LDA}}$ down to compensate for the fact that we are approximating the exact v_{xc} which has a particle number discontinuity by an approximate functional which has no derivative discontinuity [37]. Specifically,

$$v_{\mathrm{xc}}^{\mathrm{AC\text{-}LDA}}(\mathbf{r}) = \mathrm{Max}\big[v_{\mathrm{xc}}^{\mathrm{LDA}}(\mathbf{r}) - \Delta, v_{\mathrm{xc}}^{\mathrm{LB94}}(\mathbf{r})\big], \tag{1.5}$$

where

$$\Delta = I + \epsilon_{\mathrm{HOMO}} \tag{1.6}$$

is the difference between the ΔSCF ionization potential and the negative of the highest occupied molecular orbital (HOMO) energy, in the LDA. This asymptotically corrected LDA (AC-LDA) will be used in the present work (i.e., we use the TDLDA/AC-LDA functional, meaning that the AC-LDA is used for the SCF step and then combined with the TDLDA coupling in the post-SCF

step). The AC-LDA energy expression is

$$E^{\text{AC-LDA}} = \sum_i \epsilon_i - \int v_{\text{xc}}^{\text{AC-LDA}}(\mathbf{r})\rho(\mathbf{r})\,d\mathbf{r}$$
$$- \frac{1}{2}\iint \frac{\rho(\mathbf{r}_1)\rho(\mathbf{r}_2)}{r_{12}}\,d\mathbf{r}_1\,d\mathbf{r}_2 + E_{\text{xc}}^{\text{LDA}}[\,\rho\,],$$

$$(1.7)$$

and gives total energies very close to those of the LDA since $v_{\text{xc}}^{\text{AC-LDA}}$ and $v_{\text{xc}}^{\text{LDA}}$ differ by no more than a rigid shift in the energetically important regions of space [37]. Using the TDLDA/AC-LDA functional, we obtained most of the first 20–30 vertical excitations of formaldehyde and 3 other small molecules to within 0.5 eV [37]. Although there are a few states with larger errors ($\sim$ 1 eV), indicating a need for continued improvement of the functional, the results from the AC-LDA functional are good enough that we are now in a position to hope that TD-DFT will be able to describe photochemically interesting phenomena involving both valence and Rydberg excitations, and configuration mixing between the two.

As a first trial, we have chosen to focus on the CO-stretch cross section of the $^1A_1$ manifold of formaldehyde. These surfaces exhibit avoided crossings due to configuration mixing, and this mixing has been found to be essential for a resolution of the longstanding enigma of why the $^1(\pi, \pi^*)$ transition has never been observed experimentally [38–40]. As will be seen, TD-DFT is able to describe this phenomenon.

2. Computational Details

The TD-DFT calculations were performed using version 2 of our program deMon- (for "densité de Montréal") DynaRho (for "dynamic response of ρ") [41]. Version 4.0 of deMon-KS (for "Kohn–Sham") [42] was used for the SCF step due to its automated orbital symmetry assignments [43]. Both of these programs use the same auxiliary basis sets, which improve computational scaling both through the elimination of four-center integrals and by reducing the number of grid points needed to evaluate exchange–correlation terms.

Since TD-DFT produces transition densities, rather than the n-electron wave functions for the excited states, a complete assignment of term symbols for the transitions obtained typically requires

that some additional approximation be introduced. Following Ref. [30], we assume that the wave function, Ψ_I, for the Ith excited state has the form,

$$\Psi_I = \sum_{ij\sigma}^{f_{i\sigma} > f_{j\sigma}} \sqrt{\frac{\epsilon_{j\sigma} - \epsilon_{i\sigma}}{\omega_I}}\, F_{ij\sigma}^I\, \hat{a}_{j\sigma}^\dagger \hat{a}_{i\sigma}\Phi + \cdots, \quad (2.1)$$

where Φ is the single determinant of Kohn–Sham orbitals occupied in the ground-state noninteracting system and the creation and annihilation operators, $\hat{a}_{j\sigma}^\dagger$ and $\hat{a}_{i\sigma}$, refer to the Kohn–Sham molecular orbital representation. This approximation appears to be quite adequate, and is used in the present work, for the qualitative purpose of assigning term symbols to the quantitative transition energies and oscillator strengths obtained by solving the eigenvalue problem Eq. (1.3) and for analyzing the orbital promotions associated with each excitation.

We studied the CO-stretch cross section of the surfaces, holding the CH_2 moiety frozen at its experimental ground-state equilibrium geometry ($R_{\text{CH}} = 2.0796$ bohrs, $\angle HCH = 116.3°$), the same as used in Ref. [38]. The zero energy is taken to be the minimum of the ground-state CO stretching curve. The excited-state surfaces were obtained by adding the TDLDA/AC-LDA transition energy to the AC-LDA ground-state energy, for each geometry.

Gaussian-type orbital (GTO) basis sets are used for both orbital and auxiliary basis sets. We used the Sadlej+ basis set of Ref. [33], which consists of the Sadlej basis [44, 45] supplemented with two diffuse s and one set each of diffuse p and d functions, for a total of 102 contracted GTOs. The deMon library (4, 4; 4, 4) auxiliary set was used for C and O. For H, a (4, 1; 4, 1) auxiliary basis set was obtained by supplementing the deMon library (3, 1; 3, 1) basis with a diffuse s function with exponent 0.06.

The deMon "extrafine" "random" grid (with 32 radial and 194 angular points per atom) constructed using C_{2v} symmetry was used. The SCF convergence criteria were a change of less than 10^{-8} a.u. in the charge density fitting coefficients and, simultaneously, less than 10^{-8} hartree in the total energy.

3. Results and Discussion

One of the strengths of our response theory formulation of TD-DFT is that the ability to de-

scribe configuration mixing, which is important for avoided crossings, is present in the formalism. In this section, we verify that this works in practice, by comparing our TDLDA/AC-LDA excited-state surfaces with the multireference doubles configuration interaction (MRD-CI) results of Hachey, Bruna, and Grein [38] for the $^1A_1$ manifold of formaldehyde.

We will use orbital promotion labels for the primary components of the transitions in order to interpret our surfaces. Placing CH_2O in its canonical orientation [46] with CO along the z axis and the hydrogens in the (y, z) plane, DFT with the AC-LDA functional gives the following ordering of valence-type orbitals:

$$[1b_2(\sigma')]^2[5a_1(\sigma)]^2[1b_1(\pi)]^2[2b_2(n)]^2[2b_1(\pi^*)]^0,$$
$$(3.1)$$

followed by the Rydberg orbitals,

$$[6a_1(3s)]^0[7a_1(3p_z)]^0[3b_2(3p_y)]^0[3b_1(3p_x)]^0$$
$$\times \left[8a_1(3d_{x^2-y^2})\right]^0\left[4b_2(3d_{yz})\right]^0$$
$$\times[9a_1(3d_{z^2})]^0\left[1a_2(3d_{xy})\right]^0, \qquad (3.2)$$

in order of increasing energy. The ''chemical names'' are traditional [47], up to minor variations. For ease of comparison, we use the same chemical names as Hachey, Bruna, and Grein [38]. Note also that our distinction between ''valence'' and ''Rydberg'' is simply the one already well-established in the formaldehyde literature [47].

It is worthy of note that, in contrast to Hartree–Fock, all of the above unoccupied molecular orbitals are bound, and their ordering reflects the ordering of the Rydberg excited states [37]. In fact, when a sufficiently good exchange–correlation potential is used, DFT orbital energy differences provide a remarkably good approximation to Rydberg excitation energies [37, 48, 49]. This is illustrated in Table I, which also gives an idea of the level of agreement between our TDLDA/AC-LDA vertical excitation energies and the MRD-CI results of Hachey, Bruna, and Grein [38].

Since our excited-state surfaces are obtained by adding the TD-DFT transition energies to the ground-state energy, we begin with a look at our ground-state surface (Fig. 1). Note that the LDA and AC-LDA curves are virtually indistinguishable. This is as it should be, since the AC-LDA was designed to be an asymptotic correction which would leave the LDA orbitals (and hence total energy) essentially unaltered in the energetically important 'bulk' region of the molecule [37]. Although the AC-LDA and LDA curves are quite similar to the MRD-CI curve near the potential minimum, the difference increases significantly for large CO distances, where the AC-LDA and LDA curves go from being 0.1 eV too high at $R_{CO} = 2.6$ bohrs to 0.4 eV too high at 3.2 bohr. This error will be inherited by our excited-state curves. Since the error in the shape of the ground-state curve can be diminished by using a gradient-corrected functional [50], it is worth noting that the asymptotic correction paradigm applied to create the AC-LDA

TABLE I
Comparison of AC-LDA orbital energy differences, TDLDA/AC-LDA, and MRD-CI excitation energies at the experimental ground-state equilibrium geometry (R_{CO} = 2.2739 bohrs, [38, 54]).[a]

Transition	A_1 Vertical Excitation Energies (eV)		
	MRD-CI[b]	TDLDA/AC-LDA	$\Delta\epsilon$[c]
$^1(n, 3d_{yz})$	9.06 (3^1A_1)	10.13 (4^1A_1)	
$(n, 3d_{yz})$			9.76
$^3(n, 3d_{yz})$	9.18 (3^3A_1)	9.62 (3^3A_1)	
$^1(n, 3p_y)$	7.99 (2^1A_1)	8.02 (2^1A_1)	
$(n, 3p_y)$			7.99
$^3(n, 3p_y)$	7.92 (2^3A_1)	7.85 (2^3A_1)	
$^1(\pi, \pi^*)$	9.65 (4^1A_1)	9.48 (3^1A_1)	
(π, π^*)			7.42
$^3(\pi, \pi^*)$	6.15 (1^3A_1)	6.23 (1^3A_1)	

[a] Note that the $^1(n, 3d_{yz})$ and $^1(\pi, \pi^*)$ configurations are heavily mixed at this geometry (see text).
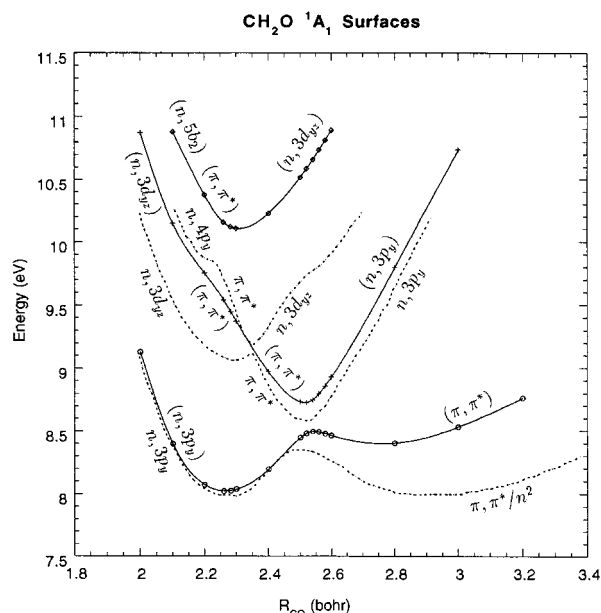[b] Refs. [38, 54], basis set B.
[c] AC-LDA orbital energy difference.

CH$_2$O Ground State Surface
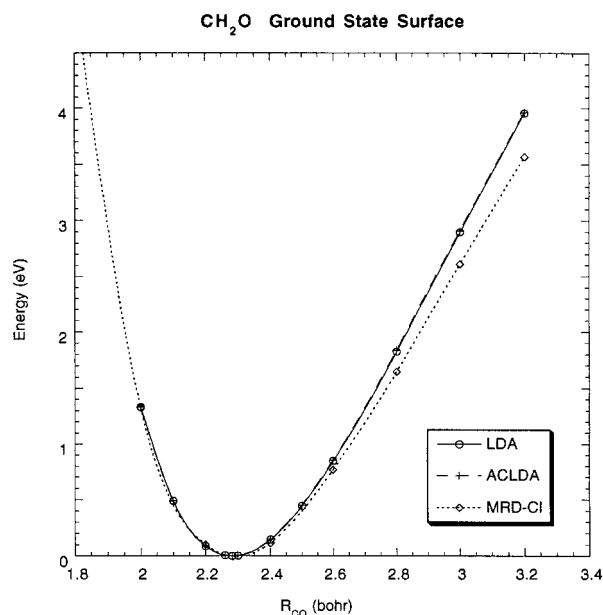
FIGURE 1. Comparison of ground-state CO-stretch potential energy curves of planar formaldehyde calculated using DFT (LDA and AC-LDA functionals) with the MRD-CI curve of Hachey, Bruna, and Grein [38] (CI data courtesy of Michel Hachey). All curves have been shifted so that their minima are at zero energy. Note that the LDA and AC-LDA curves are essentially coincident.

CH$_2$O $^1A_1$ Surfaces

FIGURE 2. Comparison of TDLDA / AC-LDA (solid) with MRD-CI [38] (dashed) 2, 3, and 4 $^1A_1$ CO-stretch potential energy curves of planar formaldehyde. The energy zeros are the minima of the corresponding (AC-LDA or MRD-CI) ground-state CO-stretch potential energy curves. The major orbital promotions found from the analysis of the TDLDA / AC-LDA "wave function" [Eq. (2.1)] have been indicated (in parentheses), as have the major orbital promotions for the MRD-CI curves given in Ref. [38] (no parentheses).

could equally well be used with a gradient-corrected functional, and would be expected to lead to improved excited-state surfaces.

The calculation of the $^1A_1$ excited-state surfaces played an important role in understanding the spectroscopy of formaldehyde. A classic puzzle has been the placement of the $^1(\pi, \pi^*)$ state. Despite an expected large oscillator strength, this transition has never been observed experimentally [38]. Hachey, Bruna, and Grein's calculation of the CO-stretch cross section of the $^1A_1$ manifold of excited-state surfaces has done much to give a definitive resolution to this enigma [38–40, 51, 52]. They found that the $^1(\pi, \pi^*)$ diabatic curve is indeed present, but that it is so strongly perturbed by Rydberg states that what is actually observed are strong mixtures of $^1(\pi, \pi^*)$ and Rydberg states. The resulting avoided crossings can be clearly understood in terms of the $^1(\pi, \pi^*)$, $^1(n, 3p_y)$, and $^1(n, 3d_{yz})$ diabatic curves (Fig. 2). (Although the diabatic curves are not shown, as such, in this figure, they are evident from the labeling of the primary components present in various portions of the adiabatic curves.) Since the $^1(\pi, \pi^*)$ diabatic curve is dissociative, Hachey, Bruna, and Grein

attribute the observed absorption continuum above about 7.5 eV to predissociating interactions. (The vertical ionization potential of CH$_2$O is 10.88 eV [53].)

This kind of global description of what is going on in the spectroscopy of the first several states in the $^1A_1$ manifold of formaldehyde is exactly the sort of information we would like to be able to obtain from TD-DFT. Our goal in the present work is not so much quantitative agreement with the MRD-CI results (since functionals for TD-DFT are still undergoing rapid development, and different basis sets are used), but rather to ascertain whether TD-DFT yields the same global picture as MRD-CI.

Figure 2 shows our TDLDA/AC-LDA excited-state CO-stretch curves. Analysis of the components of our TD-DFT excitations shows that the same three diabatic curves, $^1(\pi, \pi^*)$, $^1(n, 3p_y)$, and $^1(n, 3d_{yz})$, are present as in the MRD-CI calculation. The TDLDA/AC-LDA $^1(n, 3p_y)$ curve is within about 0.2 eV of the MRD-CI $^1(n, 3p_y)$ curve. The TDLDA/AC-LDA $^1(\pi, \pi^*)$ diabatic curve is

also close to the MRD-CI $^1(\pi, \pi^*)$ diabatic curve, for R_{CO} less than 2.5 bohrs. However, the difference increases going toward large R_{CO}, becoming about 0.7 eV at $R_{CO} = 3.2$ bohrs. This increasing error at large R_{CO} is partly due to the error in the AC-LDA ground-state surface in this region. When this is taken into account, the difference in the $^1(\pi, \pi^*)$ curves at 3.2 bohr reduces to 0.3 eV. Overall, the largest differences between the TDLDA/AC-LDA and MRD-CI diabatic curves are seen for the $^1(n, 3d_{yz})$ curves where the TDLDA/AC-LDA diabatic curve is consistently about 1 eV higher than the corresponding MRD-CI diabatic curve, though this difference reduces to 0.5 eV for small R_{CO} (2.0–2.1 bohr). Our tests at the equilibrium geometry indicate that differences in orbital basis set, and the choice of auxiliary basis, change these excitation energies only by about 0.1 eV or so. The substantial observed difference between the TDLDA/ AC-LDA and MRD-CI $^1(n, 3d_{yz})$ diabatic curves thus appears to be due primarily to limitations of the functional.

The most striking feature of the TDLDA/AC-LDA curves is the appearance of avoided crossings. Although avoided crossings can arise simply from avoided crossings of the orbital energy curves, that is not the case for the present curves. Rather, the avoided crossings seen here are due to configuration mixing between *n*-electron states. The $^1[1b_1(\pi), 3b_1(\pi^*)] / \, ^1[2b_2(n), 3b_2(3p_y)]$ avoided crossing is of this type, with

$$|3^1A_1\rangle \cong -0.79|^1[1b_1(\pi), 3b_1(\pi^*)]\rangle$$
$$+ 0.53|^1[2b_2(n), 3b_2(3p_y)]\rangle$$
$$+ 0.29|^1[2b_2(n), 4b_2(3d_{yz})]\rangle,$$
$$|2^1A_1\rangle \cong 0.40|^1[1b_1(\pi), 3b_1(\pi^*)]\rangle$$
$$+ 0.91|^1[2b_2(n), 3b_2(3p_y)]\rangle, \quad (3.3)$$

at 2.5 bohr. Because our formulation of TD-DFT is a response theory method based upon ground-state orbitals, multiconfiguration descriptions of excitations may arise both from relaxation effects and from true configuration mixing. While the combination of the last two terms in the 3^1A_1 expansion may be simply interpreted as arising from a single excitation with relaxation,

$$2b_2(n) \rightarrow 3b_2' = 0.88 \times 3b_2(3p_y)$$
$$+ 0.48 \times 4b_2(3d_{yz}), \quad (3.4)$$

and so could be described with a single excited-state configuration, $^1[2b_2(n), 3b_2']$, the presence of combinations of $b_1 \rightarrow b_1$ with $b_2 \rightarrow b_2$ terms cannot. Thus, this avoided crossing does indeed involve true configuration mixing. Note that the resulting energy separation (between the 2^1A_1 and 3^1A_1 curves) is about the same in the TD-DFT and MRD-CI results.

Examination of the components of the 3^1A_1 and 4^1A_1 states reveals strong configuration mixing of $^1(\pi, \pi^*)$ and $^1(n, 3d_{yz})$, in the region around 2.3–2.4 bohr and indicates an avoided crossing of these two curves. However, since the TDLDA/AC-LDA diabatic $^1(n, 3d_{yz})$ curve is about 1 eV higher than the corresponding MRD-CI curve, it is not surprising that the appearance of the respective avoided crossings is different. In the TDLDA/AC-LDA results, the 4^1A_1 transition at $R_{CO} = 2.1$ bohr is predominantly $^1(n, 5b_2)$, where the $5b_2$ is an unbound unoccupied orbital to which we have not attempted to assign a "chemical" name. In view of the proximity to the molecular ionization potential, the orbital and auxiliary basis sets, as well as the functional, should be further investigated before attaching too much significance to the points approaching 11 eV.

The TDLDA/AC-LDA $^1A_1$ CO-stretch curves are qualitatively similar to the MRD-CI curves, and the TDLDA/AC-LDA does yield the important mixing of the $^1(\pi, \pi^*)$ with the $^1(n, 3p_y)$ and the $^1(n, 3d_{yz})$ Rydberg excitations, thus giving the same global picture found by Hachey, Bruna, and Grein [38] to explain why the long sought $^1(\pi, \pi^*)$ transition has never been observed. A ΔSCF-based DFT study of these excited-state curves would have been far more difficult (if it were possible), involving multiple ΔSCF (or Slater transition orbital) calculations for each geometry. Even so, it is difficult to see how the extensive configuration mixing at these energies could be described by the ΔSCF-based approach without the introduction of *post hoc* second-order corrections [7] of a non-DFT nature.

4. Conclusion

In this work, we have presented the first DFT calculation of excited-state surfaces exhibiting avoided crossings. The present results with the TDLDA/AC-LDA functional show that TD-DFT is capable of describing the important configuration

mixing effects intrinsic to the behavior of these surfaces, and that TD-DFT yields the same global picture of the spectroscopy of the long-enigmatic $^1A_1$ manifold of formaldehyde as was found in the MRD-CI study of Hachey, Bruna, and Grein [38]. While the TDLDA/AC-LDA already gives a good qualitative description, and is quantitative (agreement within a few tenths of an eV) for some portions of these surfaces, further improvement in the functional will be needed in order to make the results fully quantitative.

References

1. P. Hohenberg and W. Kohn, Phys. Rev. **136**, B864 (1964).

2. W. Kohn and L. J. Sham, Phys. Rev. **140**, A1133 (1965).

3. R. G. Parr and W. Yang, *Density-Functional Theory of Atoms and Molecules* (Oxford University Press, New York, 1989).

4. R. P. Messmer and D. R. Salahub, J. Chem. Phys. **65**, 779 (1976).

5. T. Ziegler, A. Rauk, and E. J. Baerends, Theor. Chim. Acta **43**, 261 (1977).

6. C. Daul, Int. J. Quant. Chem. **52**, 867 (1994).

7. C. A. Daul, K. G. Doclo, and A. C. Stuückel, in *Recent Advances in Density Functional Methods*, *Part II*, D. P. Chong, Ed. (World Scientific, Singapore, 1997), p. 61.

8. A. Bencini, F. Totti, C. A. Daul, P. Fantucci, and V. Barone, Inorg. Chem. **36**, 5022 (1997).

9. A. Zangwill and P. Soven, Phys. Rev. A **21**, 156 (1980).

10. K. Nuroh, M. J. Stott, and E. Zaremba, Phys. Rev. Lett. **49**, 862 (1982).

11. G. Bertsch, Comp. Phys. Comm. **60**, 247 (1990).

12. M. Brack, Rev. Mod. Phys. **65**, 677 (1993).

13. A. Rubio, J. A. Alonso, X. Blase, L. C. Balbás, and S. G. Louie, Phys. Rev. Lett. **77**, 247 (1996).

14. A. Liebsch, *Electronic Excitations at Metal Surfaces* (Plenum, New York, 1997).

15. Z. H. Levine and P. Soven, Phys. Rev. Lett. **50**, 2074 (1983).

16. Z. H. Levine and P. Soven, Phys. Rev. A **29**, 625 (1984).

17. V. Peuckert, J. Phys. C **11**, 4945 (1978).

18. S. Chakravarty, M. B. Fogel, and W. Kohn, Phys. Rev. Lett. **43**, 775 (1979).

19. L. J. Bartolotti, Phys. Rev. A **24**, 1661 (1981).

20. L. J. Bartolotti, Phys. Rev. A **26**, 2243 (1982).

21. B. H. Deb and S. K. Ghosh, J. Chem. Phys. **77**, 342 (1982).

22. E. Runge and E. K. U. Gross, Phys. Rev. Lett. **52**, 997 (1984).

23. H. Kohl and R. M. Dreizler, Phys. Rev. Lett. **56**, 1993 (1986).

24. A. K. Dhara and S. K. Ghosh, Phys. Rev. A **35**, 442 (1987).

25. D. Mearns and W. Kohn, Phys. Rev. A **35**, 4796 (1987).

26. R. van Leeuwen, Phys. Rev. Lett. **80**, 1280 (1998).

27. E. K. U. Gross and W. Kohn, Adv. Quant. Chem. **21**, 255 (1990).

28. E. K. U. Gross, C. A. Ullrich, and U. J. Gossmann, in *Density Functional Theory*, E. K. U. Gross and R. M. Dreizler, Eds., NATO ASI Series (Plenum, New York, 1994), p. 149.

29. E. K. U. Gross, J. F. Dobson, and M. Petersilka, in *Density Functional Theory II*, Vol. 181 of *Topics in Current Chemistry*, R. F. Nalewajski, Ed. (Springer, Berlin, 1996), p. 81.

30. M. E. Casida, in *Recent Advances in Density Functional Methods*, *Part I*, D. P. Chong, Ed. (Singapore, World Scientific, 1995), p. 155.

31. C. Jamorski, M. E. Casida, and D. R. Salahub, J. Chem. Phys. **104**, 5134 (1996).

32. M. E. Casida, in *Recent Developments and Applications of Modern Density Functional Theory*, *Theoretical and Computational Chemistry*, *Vol. 4*, J. M. Seminario, Ed. (Elsevier Science, Amsterdam, 1996) p. 391.

33. M. E. Casida, C. Jamorski, K. C. Casida, and D. R. Salahub, J. Chem. Phys. **108**, 4439 (1998).

34. R. Bauernschmitt and R. Ahlrichs, Chem. Phys. Lett. **256**, 454 (1996).

35. R. van Leeuwen and E. J. Baerends, Phys. Rev. A **49**, 2421 (1994).

36. S. J. A. van Gisbergen, F. Kootstra, P. R. T. Schipper, O. V. Gritsenko, J. G. Snijders, and E. J. Baerends, Phys. Rev. A **57**, 2556 (1998).

37. M. E. Casida and D. R. Salahub, to appear.

38. M. R. J. Hachey, P. J. Bruna, and F. Grein, J. Phys. Chem. **99**, 8050 (1995).

39. M. R. J. Hachey and F. Grein, Chem. Phys. Lett. **256**, 179 (1996).

40. F. Grein and M. R. J. Hachey, Int. J. Quant. Chem. Symp. **30**, 1661 (1996).

41. M. E. Casida, C. Jamorski, and D. R. Salahub, deMon-DynaRho version 2, University of Montreal.

42. (a) A. St-Amant and D. R. Salahub, Chem. Phys. Lett. **169**, 387 (1990); (b) Alain St-Amant, Ph.D. Thesis, University of Montreal (1992); (c) M. E. Casida, C. Daul, A. Goursot, A. Koester, L. G. M. Pettersson, E. Proynov, A. St-Amant, and D. R. Salahub principal authors, H. Duarte, N. Godbout, J. Guan, C. Jamorski, M. Leboeuf, V. Malkin, O. Malkina, M. Nyberg, L. Pedocchi, F. Sim, L. Triguero, and A. Vela contributing authors, deMon-KS version 4.0, deMon Software, 1997.

43. Added to deMon-KS by Mats Nyberg and Lars G. M. Pettersson.

44. A. J. Sadlej, Coll. Czech. Chem. Comm. **53**, 1995 (1988).

45. A. Sadlej, Theor. Chim. Acta **79**, 123 (1991).

46. J. Chem. Phys. **23**, 1997 (1955).

47. D. C. Moule and A. D. Walsh, Chem. Rev. **75**, 67 (1975).

48. C. Filippi, C. J. Umrigar, and X. Gonze, J. Chem. Phys. **107**, 9994 (1997).

49. A. Savin, C. J. Umrigar, and X. Gonze, in *Electronic Density Functional Theory: Recent Progress and New Directions*, J. F. Dobson, G. Vignale, and M. P. Das, Eds. (Plenum, New York, 1997).

50. Unpublished calculations by the authors.

51. M. Hachey, P. J. Bruna, and F. Grein, J. Chem. Soc. Faraday Trans. **90**, 683 (1994).

52. M. R. J. Hachey, P. J. Bruna, and F. Grein, J. Molec. Spectr. **176**, 375 (1996).

53. C. R. Brundle, M. R. Robin, N. A. Kuebler, and H. Basch, J. Am. Chem. Soc. **94**, 1452 (1972).

54. P. J. Bruna, M. R. J. Hachey, and F. Grein, J. Phys. Chem. **99**, 16576 (1995).